2010

Lanthanum doped multiferroic DyFeO3: Structural and magnetic properties

Yi Du
University of Wollongong, ydu@uow.edu.au

Zhenxiang Cheng
University of Wollongong, cheng@uow.edu.au

Xiaolin Wang
University of Wollongong, xiaolin@uow.edu.au

S X. Dou
University of Wollongong, shi@uow.edu.au

Publication Details

Du, Y, Cheng, Z, Wang, XL & Dou, SX (2010), Lanthanum doped multiferroic DyFeO3: Structural and magnetic properties, Journal of Applied Physics, 107(9), pp. 1-3.

Lanthanum doped multiferroic DyFeO3: Structural and magnetic properties

Abstract
Lanthanum doped multiferroic $DyFeO_3$ was synthesized by solid state reaction. X-ray diffraction and refinement show that the lattice parameters of $Dy_{1-x}La_xFeO_3$ increase linearly with the La content. Raman spectroscopy reveals that the short-range force constant in $Dy_{1-x}LaxFeO_3$ is decreased by La^{3+} ion substitution. The spin reorientation phase transition temperature (T_{SRPT}) is observed to decrease along with the doping level. The antiferromagnetic ordering temperature T_N of Fe^{3+} ions is depressed with increasing doping level. Both decreasing T_{SRPT} and decreasing T_N indicate that Fe–Dy and Fe–Fe interactions are weakened by La substitution. It is found that the electron configuration of Fe^{3+} is high spin state and not affected by the La doping in all the samples above T_N.

Keywords
Lanthanum, doped, multiferroic, DyFeO3, Structural, magnetic, properties

Disciplines
Engineering | Physical Sciences and Mathematics

Publication Details
Du, Y, Cheng, Z, Wang, XL & Dou, SX (2010), Lanthanum doped multiferroic DyFeO3: Structural and magnetic properties, Journal of Applied Physics, 107(9), pp. 1-3.

Lanthanum doped multiferroic $DyFeO_3$: Structural and magnetic properties

Y. Du, Z. X. Cheng,[a] X. L. Wang, and S. X. Dou
Institute for Superconducting and Electronic Materials, University of Wollongong, Wollongong, New South Wales 2522, Australia

(Presented 19 January 2010; received 29 October 2009; accepted 15 December 2009; published online 3 May 2010)

Lanthanum doped multiferroic $DyFeO_3$ was synthesized by solid state reaction. X-ray diffraction and refinement show that the lattice parameters of $Dy_{1-x}La_xFeO_3$ increase linearly with the La content. Raman spectroscopy reveals that the short-range force constant in $Dy_{1-x}La_xFeO_3$ is decreased by La^{3+} ion substitution. The spin reorientation phase transition temperature (T_{SRPT}) is observed to decrease along with the doping level. The antiferromagnetic ordering temperature T_N of Fe^{3+} ions is depressed with increasing doping level. Both decreasing T_{SRPT} and decreasing T_N indicate that Fe–Dy and Fe–Fe interactions are weakened by La substitution. It is found that the electron configuration of Fe^{3+} is high spin state and not affected by the La doping in all the samples above T_N. © *2010 American Institute of Physics*. [doi:10.1063/1.3360354]

Compounds which display coexistence of magnetic and ferroelectric (*FE*) orders are known as multiferroic materials.[1] Among these materials, *FE* (anti-)ferromagnets have been extensively studied due to their possible applications in many fields,[2–4] such as nonvolatile memory devices, sensors, and actuators. However, only a very few single-phase multiferroic materials which exhibit both large electric polarization (*P*) and strong magnetoelectric (*ME*) coupling have been studied so far.[5–7] Recently, a magnetic-field-induced *FE* state has been observed in $DyFeO_3$ single crystal.[8] A large linear *ME* tensor component $\sim 2.4 \times 10^{-2}$ was found below ~4 K. It was reported that the exchange striction working between antiferromagnetically ordered Fe^{3+} and Dy^{3+} layer structures is the possible origin for the multiferroic behavior. Thus, study of the interaction between the two types of magnetic atoms (Dy and Fe) in $DyFeO_3$ is quite important to reveal the microscopic mechanism behind multiferroic behavior. As one of typical perovskite $ReTmO_3$ (*Re*: rare-earth; *Tm*: transition metal) compounds, $DyFeO_3$ crystallizes in the orthorhombic structure with space group *Pnma*. The Dy^{3+} ions are located in the space between the FeO_6 octahedra in the crystal structure. The magnetic interactions in $DyFeO_3$ should follow the hierarchy of Fe–Fe, Fe–Dy, and Dy–Dy in descending order.[9] In previous works, the magnetic structure, as well as the Fe–Dy and Dy–Dy antiferromagnetic (AFM) interactions were studied by Mössbauer spectrometry and neutron diffraction.[10,11] Generally, substitution into *Re* or *Tm* sites in $ReTmO_3$ compounds will result in modifications of the crystal structure, causing changes in the physical properties. In the case of $DyFeO_3$, doping with La^{3+} ions, which have a larger ionic radius than Dy^{3+} ions, would lead to structural distortion, which possibly alters the electronic structure and magnetic properties. In addition, the doped nonmagnetic La^{3+} ions are expected to dilute the concentration of Dy^{3+} ions, which would depress the AFM Dy–Dy and Fe–Dy interactions.

In the present work, the crystal structure, magnetic properties, and electron configuration of $Dy_{1-x}La_xFeO_3$ (x=0.0, 0.1, 0.2, 0.3, and 0.4) are investigated. The goal of this work is to provide useful information on the chemical pressure effects resulting from *Re*-site doping on the crystal structure and magnetic properties.

$Dy_{1-x}La_xFeO_3$ (x=0.0, 0.1, 0.2, 0.3, and 0.4) powder samples were prepared by solid state reaction of the ternary oxides Dy_2O_3, La_2O_3, and Fe_2O_3. The purity of all the chemicals, obtained from Sigma-Aldrich, is 99.9%. The mixtures were pressed into pellets and sintered at 1200 °C for 12 h. Then, the products were crushed, ground, pressed into pellets, and sintered again at 1300 °C for 24 h.

The crystal structures of samples were examined by x-ray diffraction (XRD; GBC Mini-Materials Analyzer), using Cu $K\alpha$ radiation at $\lambda = 1.540\,56$ Å. XRD refinement calculations were conducted via the RIETICA software package (version 1.7.7). Raman scattering measurements, with a shift ranging from 100 to 2000 cm^{-1}, were performed with a laser Raman spectrometer (HORIBA Jobin Yvon HR320) at room temperature. An Ar^+ laser with wavelength of 632.8 nm was used for excitation of the Raman signals. The magnetic measurements were carried out using a 14 T physical properties measurement system (PPMS; Quantum Design) equipped with a vibrating sample magnetometer over a wide temperature range from 2 to 700 K.

The phase and crystallinity of the as-prepared $Dy_{1-x}La_xFeO_3$ (x=0.0, 0.1, 0.2, and 0.3) samples were examined with XRD, as shown in Fig. 1. All the samples are phase-pure without any observable impurities. The diffraction patterns could be indexed with an orthorhombic perovskite structure (space group *Pnma*) according to Joint Committee on Powder Diffraction Standards Card No. 47–0069. The Rietveld XRD refinement was carried out to calculate the lattice parameters, bond lengths, and bond angles. The lattice parameters *a*, *b*, and *c* are increased along with the La doping level. Overall, the lattice expands as a result of La substitution. In addition, the distortion of Fe–O octahedra in $Dy_{1-x}La_xFeO_3$ samples is reduced with doping. The in-plane

[a]Author to whom correspondence should be addressed: Electronic mail: cheng@uow.edu.au

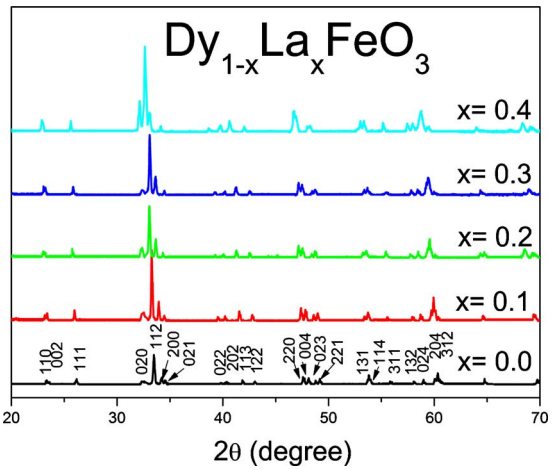

FIG. 1. (Color online) XRD patterns of $Dy_{1-x}La_xFeO_3$ (x=0.0, 0.1, 0.2, 0.3, and 0.4) samples synthesized by solid state reaction. All the peaks were indexed with JCPDS Card No. 47–0069.

Fe–O bond lengths decrease, and the out-of-plane bond lengths increase along with the doping level. Distances of the nearest Re^{3+} ions in $Dy_{1-x}La_xFeO_3$ were calculated to increase along with the x value as well. The modified crystal structure can be attributed to the different radii of the La^{3+} and Dy^{3+} ions.

Due to the relatively weak contribution to the structural factors by O^{2-} ions in the XRD analysis, some disorder effects in the anion sublattice cannot be distinguished. Therefore, Raman spectroscopy analysis of $Dy_{1-x}La_xFeO_3$ (x =0.0, 0.1, 0.2, 0.3, and 0.4) has been performed with special attention to the vibration bands that are most affected by crystal structure disorder. Figure 2 shows Raman spectroscopy results for the $Dy_{1-x}La_xFeO_3$ (x=0.0, 0.1, 0.2, 0.3, and 0.4) samples at room temperature. The irreducible representation for $DyFeO_3$ at the center of the Brillouin zone is given by

$$\Gamma = 7A_{1g} + 8A_{1u} + 7B_{1g} + 8B_{1u} + 5B_{2g} + 10B_{2u} + 5B_{3g} + 10B_{3u},$$

in which there are 24 Raman-active modes, 28 infrared modes, and 8 inactive modes.[12] In order to identify the Raman shift peaks for different samples, the $Dy_{1-x}La_xFeO_3$ Raman spectra were fitted in the range of 100–550 cm^{-1} by the Gaussian fitting method, as is shown in Fig. 2(b). There are ten vibration modes that have been identified. This agrees with results from a previous study on $DyFeO_3$ ceramics.[9] Based on a Raman study of $SmFeO_3$, the effective mass (m_{eff}),[13] which is defined as m_{eff}=x m_{La}+(1−x)m_{Dy}, is introduced for the discussion of the doping effect on the Raman shift in $Dy_{1-x}La_xFeO_3$. Most of the Raman modes above 100 cm^{-1} show a frequency decrease with the effective mass (m_{eff}) of Re^{3+} ions in $Dy_{1-x}La_xFeO_3$. Due to the systematic increase in the cell size with the decreased m_{eff} of the Re^{3+} ions, the Re−O and Fe–O force constants will be slightly decreased, which results in decreased frequency of the vibration modes. Unlike the sharp vibration peaks observed in pure $DyFeO_3$, the Raman spectra of La doped samples exhibit significantly broadened peaks. This effect is related to the disordered crystal structure induced by the La^{3+} ion substitution in $DyFeO_3$. The presence of La^{3+} in Dy^{3+} sites causes less distortion of the FeO_6 octahedra than in pure

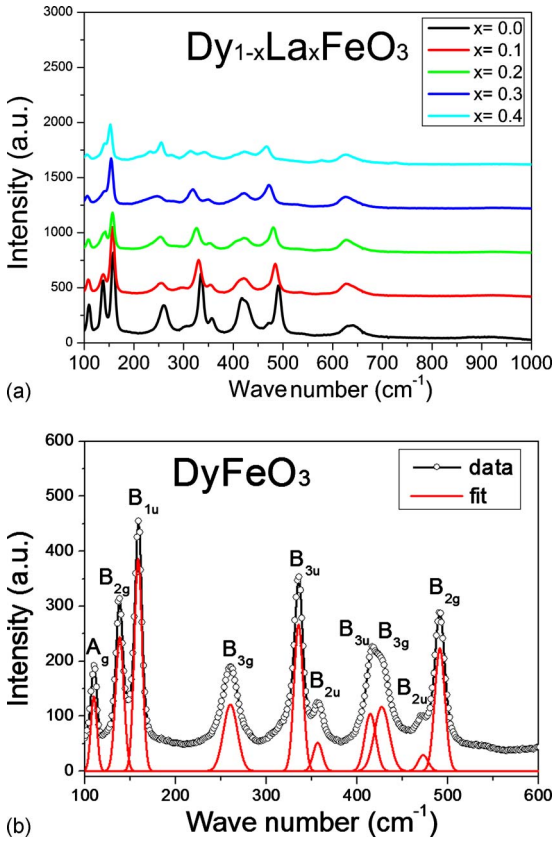

FIG. 2. (Color online) Raman spectra of $Dy_{1-x}La_xFeO_3$ collected at room temperature: (a) Raman spectra for samples with x=0.0 to 0.4. (b) Normalized Raman spectra with fitted Raman peaks for undoped specimen. The vibration modes are indexed.

$DyFeO_3$, which has been confirmed by the XRD refinement calculations. The high frequencies (>100 cm^{-1}) of these vibration modes and the broadening of the peaks should be attributed to the disordered O^{2-} ions, as well as the different masses of La^{3+} and Dy^{3+} ions.

The field cooled magnetic susceptibility (χ) as a function of temperature T from 10 to 700 K in magnetic field of H =1000 Oe is plotted in Fig. 3. The data were collected by a

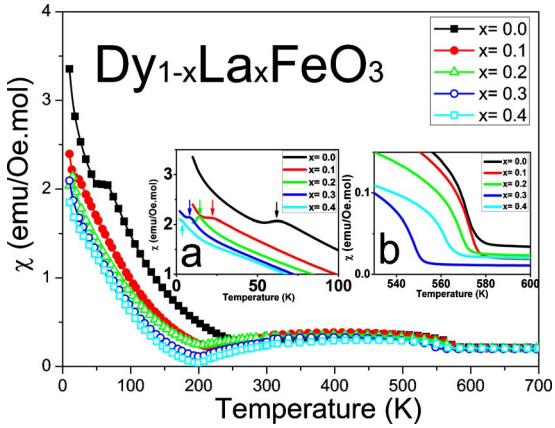

FIG. 3. (Color online) Field cooled magnetic susceptibility as a function of temperature for the $Dy_{1-x}La_xFeO_3$ (x=0.0, 0.1, 0.2, 0.3, and 0.4) samples in a magnetic field of 1000 Oe over the temperature range from 10 to 700 K. Inset (a) shows M-T curves measured from 2 to 100 K, in which T_{SRPT} decreases with increasing doping level (with T_{SRPT} indicated by the corresponding arrows). Inset (b) shows M-T curves measured in the high temperature range.

field cooling measurement on the $Dy_{1-x}La_xFeO_3$ samples. A spin reorientation phase transition (SRPT) of Fe^{3+} ions was observed at T_{SRPT}=60.1 K. It was found that T_{SRPT} decreases linearly with increasing La doping level, as shown in inset of Fig. 3(a). There are three possible Fe^{3+} spin configurations, labeled Γ_4, Γ_2, and Γ_1, which are compatible with the canting of the iron spins, the magnetic symmetry group ($m'm'm$) of these crystals, and the strong AFM coupling between nearest-neighbor Fe^{3+} sites.[14] According to a previous study,[15] $DyFeO_3$ undergoes a Γ_4-Γ_1 SRPT at T_{SRPT}. It has been proven that this temperature-induced SRPT is determined by the exchange interactions between Fe^{3+} and Re^{3+} ions in $ReFeO_3$ compounds.[9] Because the total angular momentum is J=0 for La^{3+} ions, this results in a zero magnetic moment for the La^{3+} ion. The La^{3+} substitution will reduce the contribution of Re^{3+} to the magnetic interactions in $Dy_{1-x}La_xFeO_3$ samples. Thus, the exchange interaction of Fe–Dy is weaker in doped samples, which results in decreasing T_{SPRT} with increasing content of La^{3+} ions in $Dy_{1-x}La_xFeO_3$. In addition, the magnetic moments of $Dy_{1-x}La_xFeO_3$ at T_{SRPT} decreased along with the increasing value of x, which should be ascribed to the increasing concentration of nonmagnetic La^{3+} ions. An antiferromangetic transition temperature (T_N) was observed for $Dy_{1-x}La_xFeO_3$ above 300 K. It indicates that T_N is depressed with increasing doping level. Broadening of the AFM peaks was observed due to the weaker AFM ordering in doped samples. The $Dy_{1-x}La_xFeO_3$ samples with $x \geq 0.1$ show weak ferromagnetic behavior [inset of Fig. 3(b)] in the high temperature M-T curve due to a possible canting angle arising from nearby Fe^{3+} AFM ordering [similar to the spiral magnetic structure in $BiFeO_3$ (Ref. 16)]. However, further neutron diffraction study of this material is necessary to determine its detailed magnetic structure.

Figure 4 shows the Curie–Weiss law fitting of $1/\chi-T$ from 600 to 700 K for all the samples. The total effective magnetic moments in $Dy_{1-x}La_xFeO_3$ were calculated to be 5.872 μ_B, 5.791 μ_B, 5.895 μ_B, 5.906 μ_B, and 5.210 μ_B for samples with x=0.0, 0.1, 0.2, 0.3, and 0.4, respectively, where μ_B is the Bohr magneton. Because only Fe^{3+} ions contribute to the total effective magnetic moment in $Dy_{1-x}La_xFeO_3$ above T_N, the spin state S of Fe^{3+} can be used to calculate μ_{eff} via the formula $\mu_{eff}=2(S^2+S)^{1/2}$. The Fe^{3+} ions in $Dy_{1-x}La_xFeO_3$ have five electrons in the 3d shell, which leads to a total possible spin quantum number S with values 1/2, 3/2, and 5/2. Therefore, the possible μ_{eff} are 5.916 μ_B/Fe^{3+} for the high spin state (HS), 3.873 μ_B/Fe^{3+} for the intermediate spin state, and 1.732 μ_B/Fe^{3+} for the low spin state, respectively. Compared with the results from linear fitting of the $1/\chi-T$ curves, the spin state was found to be HS for all the samples.

In summary, the effects of La doping on the structure and magnetic properties of $DyFeO_3$ have been studied. XRD refinement and Raman spectroscopy revealed that the crystal structure of $Dy_{1-x}La_xFeO_3$ (x=0.0, 0.1, 0.2, 0.3, and 0.4) is modified sequentially by the increasing La content. The vibration modes in the Raman spectra show a frequency decrease with increasing doping level in $Dy_{1-x}La_xFeO_3$, which is attributed to decreasing $Re-O$ and Fe–O force constants. The doped nonmagnetic La^{3+} ions weaken the Fe–Dy interaction in $Dy_{1-x}La_xFeO_3$, which results in a decreased T_{SRPT} and moment. The AFM temperature T_N decreases due to distorted Fe–O bond lengths, which leads to weak ordering of Fe–Fe. The electron configuration of Fe^{3+} ions is found to be HS for all the samples above T_N.

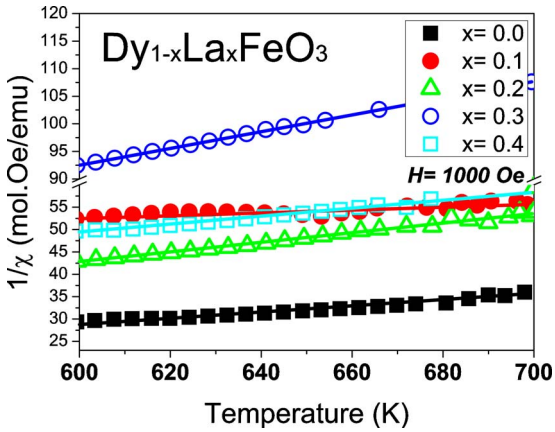

FIG. 4. (Color online) Inverse magnetic susceptibility as a function of temperature ($1/\chi-T$) and the Curie–Weiss law fittings are shown above T_N from 600 to 700 K for each sample.

This work is supported by funding from an Australian Research Council Discovery under (Project No. DP0987190). Z. X. Cheng thanks ARC for support through Future Fellowship (FT 0990287). Y. Du would like to thank the University of Wollongong for providing HDR and UPA scholarships for his Ph.D study. The authors also thank Dr. Tania Silver for her kind help in revision of the manuscript.

[1] H. Schmid, Ferroelectrics **162**, 317 (1994).
[2] N. Hur, S. Park, P. A. Sharma, J. S. Ahn, S. Guha, and S.-W. Cheong, Nature (London) **429**, 392 (2004).
[3] N. Ikeda, H. Ohsumi, K. Ohwada, K. Ishii, T. Inami, K. Kakurai, Y. Murakami, K. Yoshii, S. Mori, Y. Horibe, and H. Kitô, Nature (London) **436**, 1136 (2005).
[4] Z. X. Cheng, X. L. Wang, K. Ozawa, and H. Kimura, J. Phys. D: Appl. Phys. **40**, 703 (2007).
[5] J. Wang, J. B. Neaton, H. Zheng, V. Nagarajan, B. Ogale, B. Liu, D. Viehland, V. Vaithyanathan, D. G. Schlom, U. V. Waghmare, N. A. Spaldin, K. M. Rabe, M. Wuttig, and R. Ramesh, Science **299**, 1719 (2003).
[6] Z. X. Cheng, A. H. Li, X. L. Wang, S. X. Dou, K. Ozawa, H. Kimura, S. J. Zhang, and T. R. Shrout, J. Appl. Phys. **103**, 07E507 (2008).
[7] C. J. Fennie, Phys. Rev. Lett. **100**, 167203 (2008).
[8] Y. Tokunaga, S. Iguchi, T. Arima, and Y. Tokura, Phys. Rev. Lett. **101**, 097205 (2008).
[9] S. Venugopalan, M. Dutta, A. K. Ramdas, and J. P. Remeika, Phys. Rev. B **31**, 1490 (1985).
[10] L. A. Prelorendjo, C. E. Johnson, M. F. Thomas, and B. M. Wanklyn, J. Phys. C **13**, 2567 (1980).
[11] H. H. Schmidt, K. König, and H. Daniel, Acta Crystallogr., Sect. A: Found. Crystallogr. **39**, 682 (1983).
[12] H. C. Gupta, M. K. Singh, and L. M. Tiwari, J. Raman Spectrosc. **33**, 67 (2002).
[13] E. Traversa, P. Nunziante, L. Sangaletti, B. Allieri, L. E. Depero, H. Aono, and Y. Sadaoka, J. Am. Ceram. Soc. **83**, 1087 (2000).
[14] R. L. White, J. Appl. Phys. **40**, 1061 (1969).
[15] V. V. Eremenko, S. L. Gnatchenko, N. F. Kharchenko, P. P. Lebedev, K. Piotrowski, H. Szymczak, and R. Szymczak, Europhys. Lett. **4**, 1327 (1987).
[16] J. F. Scott, M. K. Singh, and R. S. Katiyar, J. Phys.: Condens. Matter **20**, 322203 (2008).